Marine Geology 385 (2017) 56–67

Contents lists available at ScienceDirect

Marine Geology

journal homepage: www.elsevier.com/locate/margo

Late Holocene erosion of the Canopic promontory (Nile Delta, Egypt)

Clément Flaux [a], Nick Marriner [b,*], Mena el-Assal [c], David Kaniewski [a,d], Christophe Morhange [e]

[a] CNRS, EcoLab (Laboratoire d'Ecologie Fonctionnelle et Environnement), Toulouse, France
[b] CNRS, Laboratoire Chrono-Environnement UMR 6249, MSHE Ledoux, USR 3124, Université de Bourgogne-Franche-Comté, UFR ST, 16 Route de Gray, 25030 Besançon, France
[c] King Khalid University, 1, Guraiger, Abha 62529, Saudia Arabia
[d] Université Paul Sabatier-Toulouse 3, EcoLab (Laboratoire d'Ecologie Fonctionnelle et Environnement), Toulouse, France
[e] Aix-Marseille University, CEREGE, IUF, Aix-en-Provence, France

ARTICLE INFO

Article history:
Received 7 July 2016
Received in revised form 16 November 2016
Accepted 17 November 2016
Available online 22 November 2016

Keywords:
Holocene
Delta
Lobe
River mouth
Sea level
Subsidence
Sedimentary budget
Geomorphology
Geoarcheology
Human paleogeography
Herakleion
East-Canopus
Nile
Egypt

ABSTRACT

The mouths of the Nile Delta are sensitive coastal areas, their geomorphology primarily being mediated by relative sea-level rise and sediment supply. To further document the Holocene evolution of the Nile's Canopic mouth, a core was taken from the southern shores of Abu Qir Bay, close to the ancient Canopic channel. Core bio-sedimentology and chronostratigraphy highlight four stages of marine incursion which are juxtaposed upon the general progradation trend of the Nile coast in this area. Compiled age-depth points from sediment cores taken in Abu Qir Bay underscore two phases of negative sediment budget at the Canopic mouth: (1) a first period, between 3.5 and 2 ka cal. yr BC, probably in relation to the well-documented mid-to-late Holocene decline in Nile flow; and (2) a second phase, after 0.5 ka cal. AD, linked to a decline in Canopic sediment supply to the coastal area, and concomitant with the development of the Rashid branch. The erosion and reworking of material flattened and lowered the promontory surface by up to 4 m. The submersion of the Canopic promontory was completed by relative sea-level rise, primarily controlled by the compaction and liquefaction of unconsolidated lagoonal muds. The lowering of the Canopic mouth led to the submersion of two ancient estuarine-harbor cities, known as East-Canopus and Herakleion, whose remains lie 4–7 m below present mean sea level. It is argued that the subsidence of the two cities cannot explain their abandonment during the late 7th–early 8th century AD, taking into account the regional occupation pattern during Antiquity. Rather, the longevity of the two cities, spanning more than 13 centuries, shows that adaptation to coastal risks including erosion, subsidence and high-energy events like storms or tsunamis, was the rule.

1. Introduction

Human populations living on deltaic coasts are increasingly vulnerable to flooding, primarily mediated by a combination of rising relative sea level and decreasing sediment supply to coastal depocenters (Anthony, 2009; Anthony et al., 2014). The relative contribution of present global sea-level rise (1.8 mm yr^{-1}; Church et al., 2011) is now considered to be minor when compared to local subsidence processes and reduced deltaic plain aggradation (Syvitski et al., 2009; Stewart and Morhange, 2009). The Nile delta is a prime example of a coastline prone to sinking and its vulnerability has been regularly underlined by scholars (e.g. Stanley and Warne, 1993; Stanley et al., 2001; J.-D. Stanley et al., 2004; Nicholls et al., 2007; Syvitski et al., 2009; Frihy et al., 2010; Marriner et al., 2013). In particular, the Nile's promontories appear to be very sensitive (Frihy and Lawrence, 2004). Modern subsidence rates, estimated using radar interferometry data on the Damietta promontory, are as high as 6–8 mm yr^{-1}, while values of 0–5 mm yr^{-1} have been measured on the adjacent delta plain (Becker and Sultan, 2009). Between 1922 and 2000, the western Rashid promontory retreated at a mean rate of 43 m yr^{-1} (Frihy and Lawrence, 2004), reaching a peak of 100 m yr^{-1} between 1971 and 1990 (Frihy and Komar, 1993). The transition from a state of accretion to erosion occurred in the early 20th century, when sediment delivery to the mouth declined sharply, due to the Nile's upriver dams (Frihy and Lawrence, 2004) and the very dense canal and drainage network acting as a huge sedimentary trap (Stanley, 1996).

Older deltaic promontories provide the opportunity to analyze the sensitivity of these coastal features to long-term changes in Nile sediment supply. Among the seven mouths of the Nile reported in Antiquity (Toussoun, 1922, 1926), only two are still active at present (Rashid and Damietta). The others have been buried below lagoon muds (eastern delta) or eroded and reworked along beach ridges (western and northern delta) (Stanley and Warne, 1993). Nile promontories are thus short-lived deltaic depocenters at the late-Holocene timescale. Because the geomorphological response of the modern Rashid and Damietta mouths to Nile hydro-sedimentary changes has been severe, it is hypothesized that the reconstruction of past promontory evolution can help to

* Corresponding author.
E-mail address: nick.marriner@univ-fcomte.fr (N. Marriner).

http://dx.doi.org/10.1016/j.margeo.2016.11.010
0025-3227/

document the history of Nile inputs to the coast during historical times (e.g. in the Mississippi delta, see Coleman et al., 1998).

This paper details the example of the Canopic mouth, the downstream termination of the Nile delta's largest branch during Antiquity, and a key freshwater resource and navigation channel for the whole region of ancient Alexandria. Geomorphological processes shaping the evolution of the mouth are discussed in the light of detailed bio-sedimentological data of core M57 taken at the inlet of the present Edku lagoon, close to the former Canopic channel, and a review of geomorphic, archeological and historical indicators for the bay's evolution, based on previous studies. Finally, we consider the abandonment of the harbor cities of Herakleion and East-Canopus, located at the Canopic mouth, not only with regards to coastal hazards, but also in relation to the regional-scale geography of human occupation during Antiquity. The originality of the Canopic promontory, occupied from the 7th century BC to the 7th century AD, provides an excellent "cautionary tale" and relevant case-study example for the present-day evolution of urbanized deltaic mouths (Stanley et al., 2004).

2. Geomorphological setting of Abu Qir Bay

Abu Qir Bay has a concave shoreline morphology, which extends from a late Pleistocene carbonate ridge on its western side (Abu Qir headland) to the clastic promontory of Rashid in the east (Fig. 1). The bay formed during the last 1500 years, as a result of the lowering of the paleo-Canopic promontory, down to 5–7 m below MSL, and the accretion of the Rashid mouth (Chen et al., 1992; Stanley et al., 2004).

In the western part of Abu Qir Bay, underwater archeological exploration has elucidated two ancient harbor cities, located in the estuary of the Canopic branch, known as East Canopus and Herakleion in historical sources (Toussoun, 1934; Goddio, 2007). These impressive archeological remains broadly lie 4 to 7 m below present MSL and underscore the

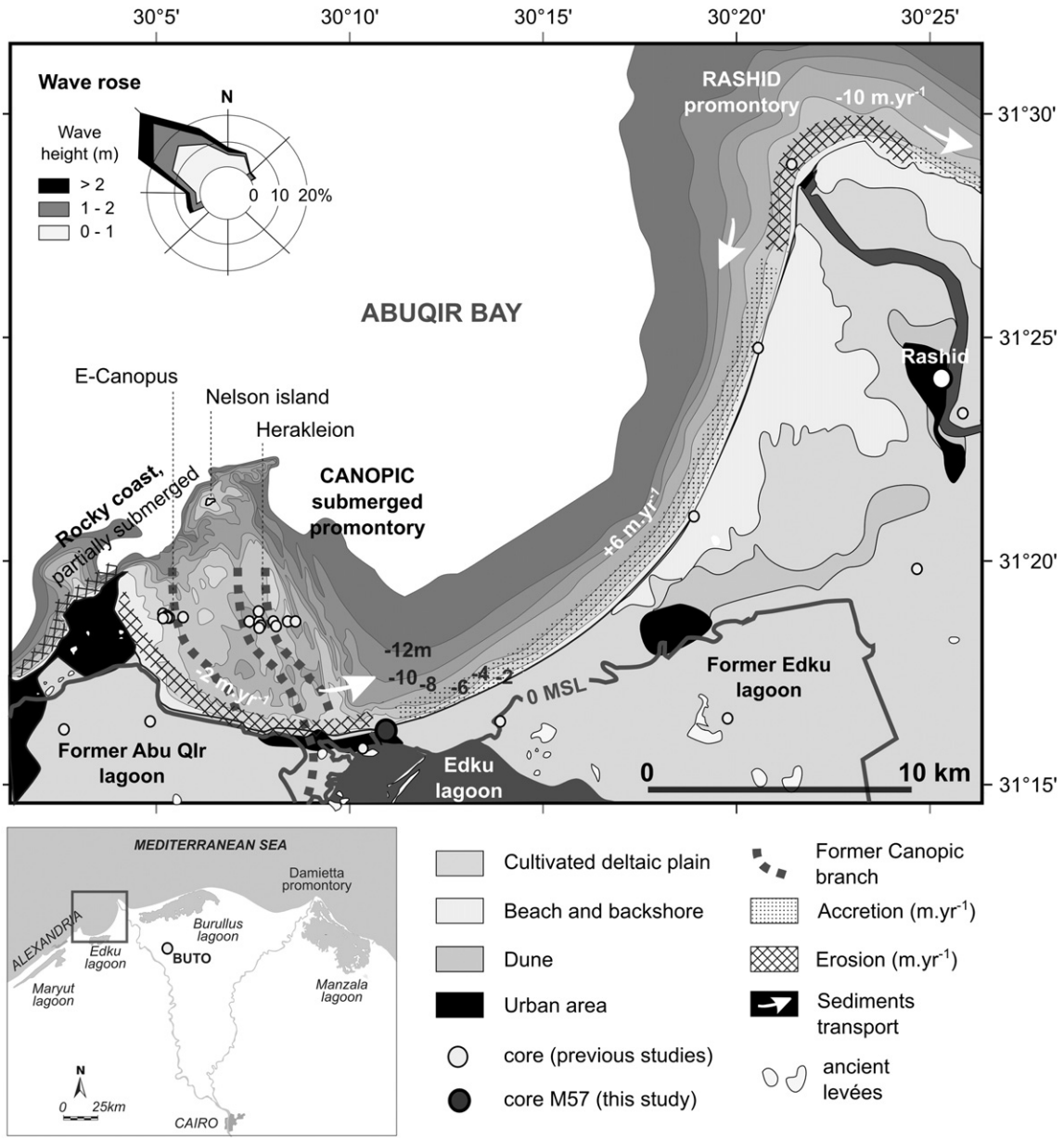

Fig. 1. Location map showing the main geomorphic features of Abu Qir Bay/Canopic coast on the western Nile delta. The bathymetry of the western bay and the positions of Herakleion and East Canopus are adapted from Goddio (2007). The spatial pattern of coastal accretion and erosion is adapted from Frihy and Komar (1993). The location of previous cores has been adapted from Stanley et al. (2007 for underwater cores; 1996). The wave rose is adapted from Frihy and Dewidar (2003).

vulnerability of coastal settlements during historical times. A combination of factors have been proposed to explain the land lowering of the Canopic coast, including tectonic re-adjustement of strata at depth, sediment compaction, growth faulting and soft sediment deformations under large anthropogenic structures, possibly triggered by earthquakes, tsunamis, Nile floods and winter storm surges (Stanley et al., 2001, 2007; J.-D. Stanley et al. 2004; Stanley, 2005a, 2005b; Stanley and Toscano, 2009). To date, however, the precise quantification of these possible forcing factors has not been probed.

According to Islamic tradition, the city of Rashid was founded in 870 AD and at this time lay at the river mouth (Wilson, 2012; Fig. 1). Consistently, archeological surveys in the area have not revealed any sites from Antiquity north of Rashid (Wilson, 2012). On Forlani's map of 1566, Rashid still lay on the coast (Stanley et al. 2004, their Fig. 4b, p. 925). It is suggested that the mouth prograded significantly into the sea after this time. Sand flats and barchan dunes separate Abu Qir Bay from Edku lagoon to the south and south-east, supplied both by inputs from the mouth and eroded material from the western Abu Qir shores (Fig. 1). Since the early 20th century, construction of seven dams along the Nile (Frihy and Lawrence, 2004) and sediment entrapment on the delta plain (Stanley, 1996) have virtually cut off sediment delivery to the Rashid mouth and induced a continuous retreat of the promontory, at a mean rate of 43 m yr^{-1} between 1922 and 2000 (Frihy and Lawrence, 2004). The rapid erosion of the Rashid promontory suggests that the geomorphology of the bay is primarily controlled by sediment flux and longdrift transport along the Abu Qir coast, while, by contrast, submerged archeological indicators highlight subsidence processes. Our goal is to further document the Holocene aggradation and degradation stages of the Canopic mouth.

3. Methods and data

Core M57 was drilled in 2009, on Idku lagoon's northern shores, at the entrance of its modern marine inlet (Fig. 1). The core surface was at the lagoon level and it is assumed that the core surface can be related to mean sea level with an error of ±0.5 m. Sedimentological descriptions were undertaken during fieldwork. A series of 45 samples, 150 to 200 g in weight, were taken along the 10-m-long sediment sequence. We performed standard bio-sedimentological analyses at the CEREGE laboratory (France). The sediment aggregates were wet sieved through meshes to separate out the gravels (>2 mm), coarse sands (0.5–2 mm), medium sands (0.2–0.5 mm), fine sands (0.063–0.2 mm), and silts and clays fractions. The resulting dry fractions were subsequently weighed and data was plotted against stratigraphic logs in percentages. In sand-rich facies, the sand fraction was subjected to mechanical sieving using a column of sieves descending in size from 1.6 mm to 0.063 mm, to construct histograms and grain-size indices. Here, we used the sorting index defined by Folk (1966). In sand-rich facies, the mean grain size and sorting index of the sandy fraction were measured and compared with modern analogues taken in Abu Qir Bay (El-Banna, 2008; Frihy et al., 1999, 2007). Identified mollusc and ostracod shells were assigned to assemblages according to the Péres and Picard (1964), Pérès (1982), Poppe and Goto (1991, 1993), and Doneddu and Trainito (2005) classification systems, as well as modern faunal groups observed on the Nile coast (Bernasconi and Stanley, 1994). Loss on ignition (LOI) was performed to estimate the organic and carbonate content of sediments, based on Heiry et al. (2001). Bulk sediment samples were heated to 550 °C to determine the relative organic matter content, and to 950 °C to establish the relative carbonate content. Magnetic susceptibility measurements were undertaken using a Bartington MS2 Magnetic Susceptibility meter, to further characterize the lithostratigraphy and sediment composition. Frihy et al. (2007) have previously shown that the distribution of magnetic minerals mapped on the seabed of Abu Qir Bay is primarily controlled by sediment transport patterns and sorting processes. The sediment samples were placed in pre-weighed 10 ml plastic cubes and oven dried for 48 h. Magnetic susceptibility (MS) was measured three times on each sample, both at low and high frequency. Samples and cubes were reweighed and the mean MS value was corrected to account for mass differences. Measurements are reported as mass-specific magnetic susceptibility in SI units ($\times 10^{-8}$ $m^3.kg^{-1}$). Linear detrended cross-correlation analyses were used to detect and quantify links and potential lags between the bio-stratigraphic time-series.

A chronology for the sequence is provided by 11 radiocarbon dates, calibrated using IntCal09 (Reimer et al., 2009; Table 1). A reservoir age of 400 years was used for shell samples, based on the radiocarbon age of a modern pre-bomb marine specimen collected live in Alexandria (Goiran, 2001). The same procedure was used to calibrate the compiled radiocarbon dataset displayed in Fig. 5. Additional age control was provided by comparison with previously published radiocarbon data and environmental changes attested at the regional scale. Ages are displayed in calibrated years BC/AD for further comparisons with the historical and archeological chronology.

Core M57 was compared and contrasted with available bio-sedimentary records in Abu Qir Bay (Stanley, 2007; Goddio, 2007). 58 radiocarbon ages were used to calculate the probability density function (PDF) of ^{14}C dates (n = 58), to detect phases of apparent sedimentary hiatus with known a depositional context. Cumulative PDFs have been widely used to synthesize radiocarbon datasets in fluvial geomorphology (e.g. for the Nile basin, Marriner et al., 2012b; Macklin et al., 2015), where probability peaks are taken to be representative of hydrogeomorphological changes.

4. Results: bio-sedimentology of core M57

The retrieved core M57 was 10 m long. Sand texture, loss on ignition, magnetic susceptibility, faunal assemblages and radiocarbon analyses have allowed nine different units to be elucidated, described below from bottom to top.

Table 1
Core M57 radiocarbon dates and calibrations (Reimer et al., 2009). 'Sac' denotes Saclay (France) and 'Beta' denotes Beta-Analytic (USA).

Code	Depth (m)	Sample	δ13X	Radiocarbon age	Age cal. BC/AD
SacA 16152	0.7	Rich organic bulk	−17.40	1630 ± 30	440 ± 90
SacA 16153	1.1	Valves of *Cerastoderma glaucum* and *Abra tenuis*	1.10	3020 ± 30	800 ± 30
Beta – 406935	2.1	Seeds	−11.7	1950 ± 30	45 ± 80
SacA 16154	2.2	Valves of *Abra tenuis*	−1.80	2005 ± 30	470 ± 70
SacA 16155	2.8	Peat sediment	−21.80	4450 ± 30	3130 ± 190
SacA 16156	4	Valves of *Cerastoderma glaucum*	−1.20	2570 ± 30	−240 ± 120
SacA 16157	5.1	Valves of *Cerastoderma glaucum*	0.90	3125 ± 30	−870 ± 60
SacA 16158	5.6	Peat sediment	−22.70	4570 ± 30	−3300 ± 190
SacA 16159	6.5	Carbonized wood	−29.40	7010 ± 35	−5900 ± 90
SacA 16161	6.6	Carbonized wood	−28.60	15,240 ± 70	−16,430 ± 310
SacA 16162	7.8	Carbonized wood	−19.00	6090 ± 35	−5030 ± 180

4.1. Unit 1

The first unit recorded developed between −10 and −7.8 m below the surface. It comprises light gray sands, dominated by medium sands from −10 to −8.5 m, and fine sands between −8.5 and −7.8 m. The sorting index varies from 0.8 to 0.5, indicating that the sands are moderately to moderately well sorted. LOI at 550 °C and at 950 °C testify to low organic matter and carbonate content, each <5% of the total sediment aggregate. The same proxies measured in fine and medium sands display similar results, except for one medium sands sample, in which carbonate content was higher than 10%. Magnetic susceptibility values in bulk and fine sands range between 15 and 95.10^{-8} m^3/kg^{-1}. The faunal content is dominated by lagoonal macrofauna (95%), namely *Hydrobia* sp., *Cerastoderma glaucum* and *Abra tenuis*, with consistently high faunal densities of the euryhaline ostracod *Cyprideis torosa* (up to 600 individuals per gram of bulk sediment). The dominant lagoonal assemblage is accompanied by minor abundances of other nearshore species, represented by *Loripes lacteus*, *Rissoa* spp., *Bittium reticulatum*, *Nassarius* sp., *Donax semistriatus*, and *Mytilaster minimus* (Fig. 3).

4.2. Unit 2

The second unit comprises gray to yellow sands, deposited between −7.8 m and −7 m. The sands grain-size frequency plot displays a well-defined mode around 200 μm and the sorting index attest to well to very well-sorted sediments. Observations under binocular microscope show that the sands are mostly quartz, often with oxidized stains. Two centimetric mud layers were found intercalated within the sandy facies at −7.8 and −7.7 m. A carbonized wood fragment found within the first mud layer was radiocarbon dated to 5030 ± 180 cal. yr BC. Organic and carbonate content remains low, each below 5% of the sediment aggregate. Magnetic susceptibility values in bulk and fine sands range between 7 and 23.10^{-8} m^3/kg^{-1}. Samples from this unit were nearly devoid of fauna, with the exception of rare specimens of *Hydrobia* sp. and a few tens of the ostracod species *Cyprideis torosa*.

4.3. Unit 3

The third unit is characterized by gray sandy muds, deposited between −7 and −6.3 m. Organic and carbonate content remains below 5%. Magnetic susceptibility values increase in this unit, between 50 up to 160.10^{-8} m^3/kg^{-1}. Faunal assemblages display similar trends to unit 1, dominated by lagoonal species (>95%) with minor abundances of coastal individuals (Fig. 3). Two carbonized wood fragments were sampled at −6.6 and −6.5 m and respectively radiocarbon dated to 16,430 ± 310 and 5900 ± 90 cal. yr BC.

4.4. Unit 4

This facies comprises black peaty muds, deposited between 6.3 and 5.5 m, best characterized by a strong enrichment of organic content from 15 to 50% of the bulk sediment. Similar values were measured in the fine sand fraction. Carbonate content increases slightly up the unit, from 2 to 7% of the sediment aggregate. The sediment texture is dominated by fine-grained mud sediments, in addition to 10–25% of coarse sand, mainly represented by organic fragments. Magnetic susceptibility values are low, between 5 and 15.10^{-8} m^3/kg^{-1}. Peat sediment sampled towards the top of the unit was radiocarbon dated to 3300 ± 190 cal. yr BC.

4.5. Unit 5

Unit 5 comprises dark gray shelly muds, deposited between 5.5 and −5 m. The bulk texture is dominated by muds (65–80%), followed by sands (10–20%) and gravels (5–10%). The unit is characterized by a marked increase in carbonate content, reaching 15% of the bulk sediment. Indeed, the sands and gravels are rich in shells, as confirmed by the carbonate content measured in the fine and medium sands, respectively reaching 20 and >30%. Shell content is represented by well-preserved individuals of *Hydrobia* sp. (>130 individuals per 10 g. of sediment), *Cerastoderma glaucum* and *Abra tenuis*. In this facies, the abundance of the ostracod *Cyprideis torosa* abundance reaches 3500 individuals per 1 g of sediment. The lagoonal assemblage (>98%) is completed by minor abundances of coastal species (Fig. 3). Some specimens of *Cerastoderma glaucum*, sampled at −5.1 m were radiocarbon dated to 870 ± 60 cal. yr BC. Organic content comprises ca. 7% of the bulk sediment and susceptibility values are low, between 15 and 30.10^{-8} m^3/kg^{-1}.

4.6. Unit 6

Unit 6 constitutes 2.5 m of homogeneous gray muds, with faintly visible laminations in some parts of the facies. Silt and clay comprise >95 to 80% of the bulk sediment from base to top unit. Organic and carbonate content remains stable throughout the unit, respectively 5 and 2% of the bulk sediment. Shell content is nearly nil, characterized by a few individuals of *Hydrobia* sp. and *Cyprideis torosa*. The magnetic susceptibility of aggregate sediment shows higher values measured in core M57, between 200 and 430.10^{-8} m^3/kg^{-1}. This parameter also increases in the sands fraction, reaching 100.10^{-8} m^3/kg^{-1}. Observation under a binocular microscope shows that the sand fraction is dominated by mica minerals. *Cerastoderma glaucum* shells were found at −4 m and radiocarbon dated to 3130 ± 190 cal. yr BC.

4.7. Unit 7

Unit 7 mainly comprises gray muds, although sand content increases, as does the gravels fraction. The unit occurs between −2.5 and −2 m. Organic content increased slightly, up to 10%. Carbonate content also increases, reaching 10% in the sediment aggregate and 18% in fine sands. Carbonates are mainly biogenic in origin, represented by the high density of *Cyprideis torosa* (up to 5000 individuals per 1 g of sediment) and *Hydrobia* sp. (up to 500 individuals per 10 g of sediment). Macrofauna is dominated by lagoonal fauna (>90%), associated with coastal species (Fig. 3). Magnetic susceptibility values decrease down to 70.10^{-8} m^3/kg^{-1}. Some valves of *Abra tenuis* sampled at −2.2 m provided a radiocarbon age of 470 ± 70 cal. yr AD. Seeds sampled at −2.1 m yielded an age of 45 ± 80 cal. yr AD.

4.8. Unit 8

This unit shows the same features as Unit 6, both in term of its texture, organic and carbonate content, magnetic susceptibility and faunal content. It appears that Units 6 and 8 were deposited under similar environmental conditions, interrupted by the deposition of Unit 7.

4.9. Unit 9

The last unit was recorded from −1.5 to −0.6 m and comprises fine gray sands intercalated with two organic-rich centimetric layers at −1.1 and −0.7 m. The texture is dominated by fine sand (>50%), followed by silt and clay (25–30%) and coarse sand and gravel (6–12%). The deposit is moderately well sorted according to the sand sorting index (Fig. 2). Organic content is below 5%, except for the rich-organic fine layers. Magnetic susceptibility oscillates between 20 and 150.10^{-8} m^3/kg^{-1}. Carbonate content in the sediment aggregate and fine sand is below 5%, however it reaches 20% in medium sand, linked to an increase in the biogenic component. The latter is once again strongly dominated by the same lagoonal species (>93%), associated with minor abundances of coastal species from various habitats (Fig. 3). Abundances of *Cyprideis torosa* and *Hydrobia* sp. present high values, respectively up to ca. 10,000 individuals per gram and 250

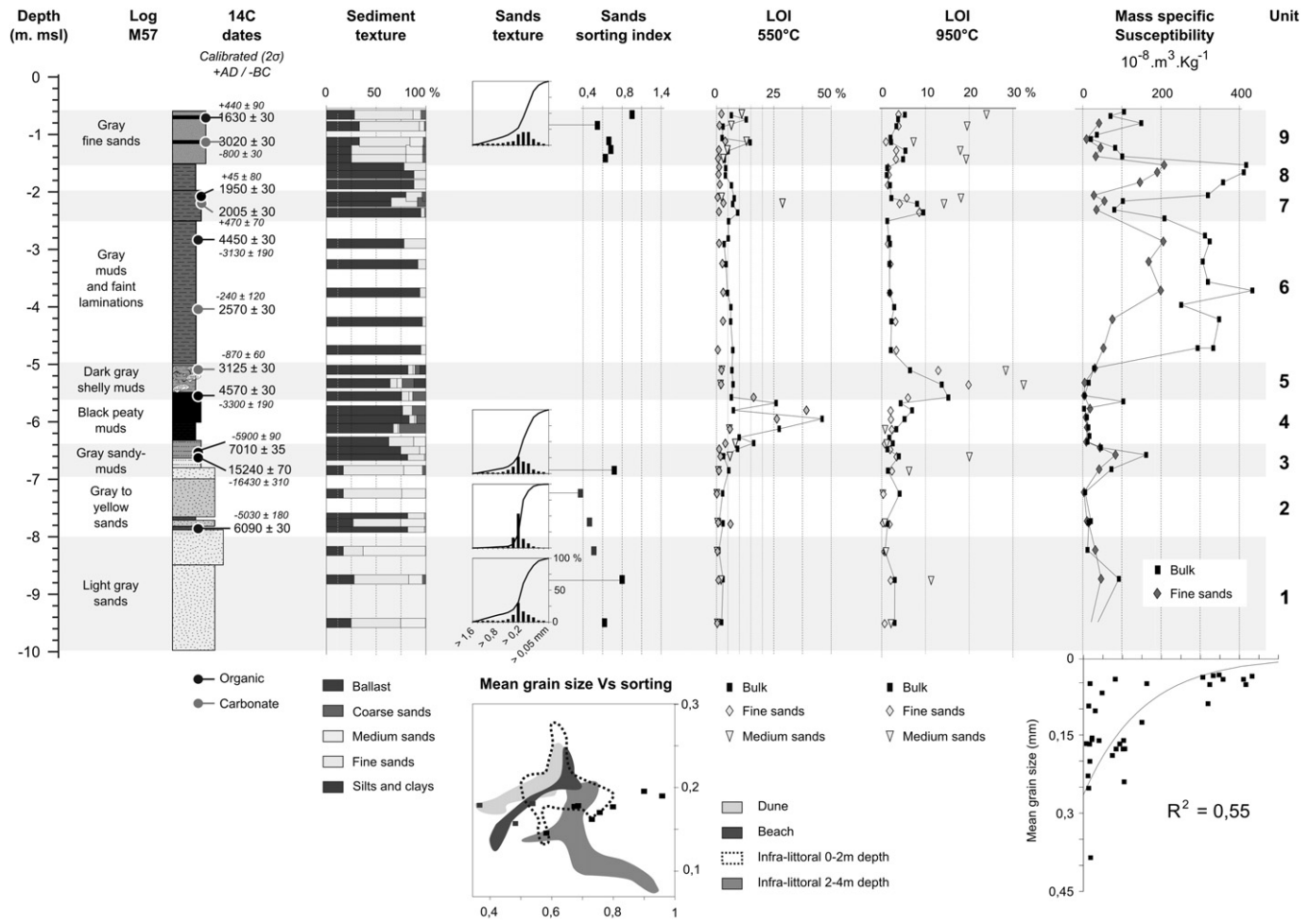

Fig. 2. Sedimentology of core M57, including grain size, sorting index, loss on ignition (LOI) at 550 °C (organic matter) and 900 °C (carbonate content), and mass specific magnetic susceptibility. Both uncalibrated and calibrated radiocarbon dates are denoted.

individuals per 10 g. Some *Cerastoderma glaucum* and *Abra tenuis* shells, sampled at −1.1 m, were radiocarbon dated to 800 ± 30 cal. yr BC. Organic sediment sampled in the upper organic-rich layer was radiocarbon dated to 440 ± 90 cal. yr AD.

5. Discussion

5.1. Holocene coastal changes recorded by core M57

5.1.1. Age model

Eleven radiocarbon-dated samples were taken from various depths, and displayed a wide chronological range spanning from 16,500 cal. yr BC to 500 cal. yr AD (Table 1). Three age-inversions were found at −6.6 m, 2.9 m and 1.1 m depth, where ages appear older than lower dated samples (Figs. 2 and 3). Carbonized wood samples taken at a similar depth in Unit 3 were respectively dated to ca. 15,200 and 5900 uncalibrated years BP (Table 1). This pre-Holocene sample is clearly reworked because: (1) all coastal sequences in the Nile delta are younger than 8000 years BP (Stanley and Warne, 1994); and (2) the marine lagoon identified in Unit 3 is inconsistent with a relative sea-level of −120 m ca. 16,500 cal. yr BC (e.g. Vacchi et al., 2016). Thus, both dates from Unit 3 were considered as reworked and removed from the M57 age model. The shelly marine lagoon muds from Unit 5 provide a chronological marker, because a similar biofacies was found in 20 sediment cores from the Abu Qir and Maryut lagoons (Flaux et al., 2011). This biofacies comprises mud deposits with 15–30% coarse biogenic sands and gravels, with the dominance of *Cyprideis torosa*, *Hydrobia* sp. and *Cerastoderma glaucum*. The unit was deposited between 3500 and 800 cal. yr BC, based on 10 radiocarbon-dated samples taken at the upper and lower boundaries of the unit (Flaux et al., 2013). This biofacies is very close to Unit 5 of core M57, the latter of which was also dated between 3500 to and 800 cal. BC. The two inverted dates in the upper sequence, with ages of 3130 ± 190 (−2.8 m, upper Unit 6) and 800 ± 30 (−1.1 m, Unit 9) cal. yr BP, were thus considered to be old reworked material. They were subsequently removed from the age model of core M57 (Fig. 4). Mean sedimentation rates subsequently calculated along core M57 were as follows: 1.3 mm.yr^{-1} between −7.8 and −5.6 m, 0.2 mm.yr^{-1} between −5.6 and −5.1 m, 1.7 mm.yr^{-1} between −5.1 and −4 m, 6.7 mm.yr^{-1} between −4 and −2.1 m and 3.5 mm.yr^{-1} between −2.1 and −0.7 m.

5.1.2. Interpretation of the faunal assemblages

Faunal assemblages are mainly dominated (90–99%) by lagoonal species, including the ostracod *Cyprideis torosa*, the gastropod *Hydrobia* sp., and the molluscan bivalves *Cerastoderma glaucum* and *Abra tenuis*. Other species (1–10%) derive from nearshore coastal areas (Fig. 2). However, there are great disparities in the diversity and abundance of species in the record. In Units 1, 3, 5, 7 and 9, high abundances of *Cyprideis torosa* and *Hydrobia* sp. were found (thousands to hundreds of individuals per 1–10 g of samples, respectively). *Cerastoderma glaucum* and *Abra tenuis* were also present in significant numbers, with minor percentages of various other coastal marine species. By contrast, intercalated Units 2, 4, 6 and 8 are characterized by the quasi-

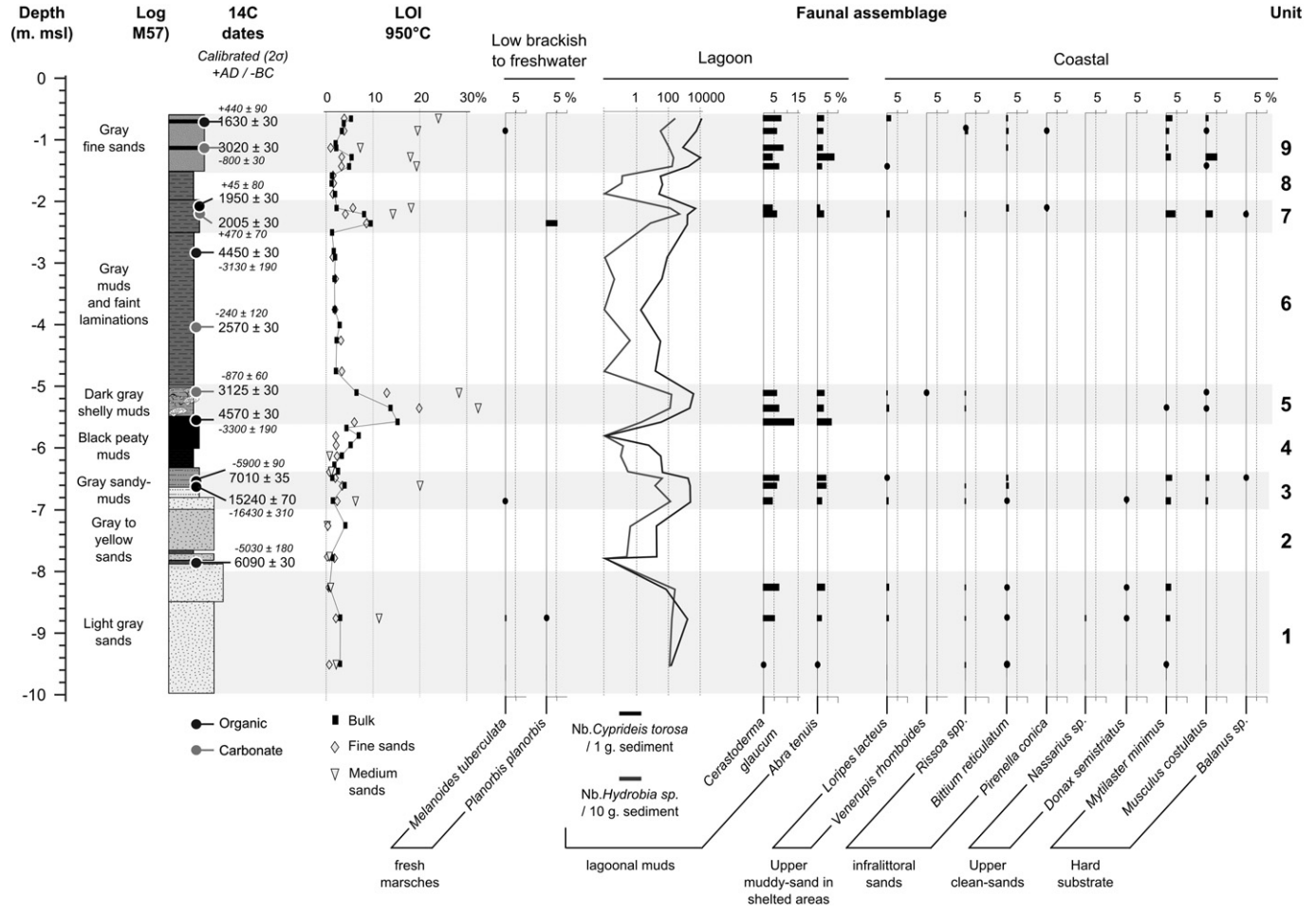

Fig. 3. Bio-stratigraphy of core M57, including loss on ignition (LOI) at 950 °C (carbonate content) and faunal assemblages. Both uncalibrated and calibrated radiocarbon dates are denoted.

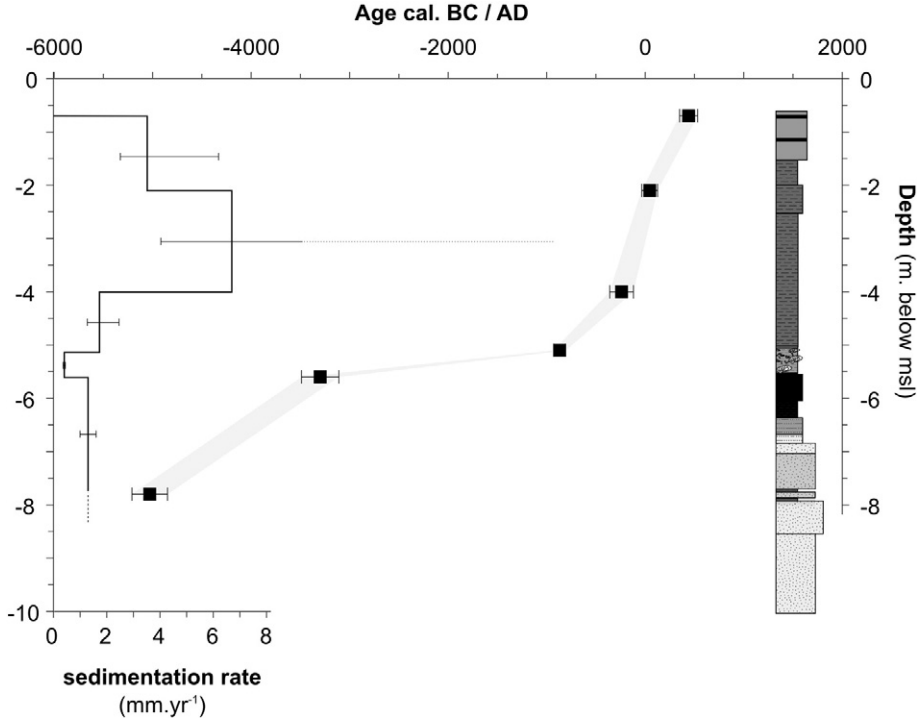

Fig. 4. Age model and sedimentation rate for core M57.

absence of fauna, with the exception of some rare specimens of *Cyprideis torosa* and *Hydrobia* sp. (Fig. 2).

Bernasconi and Stanley (1994) have defined three main molluscan clusters based on 78 surface samples taken in Nile delta lagoons: (1) lagoons with marine influence (>80% of marine species); (2) lagoonal sensu stricto (>70% of lagoonal species, primarily dominated by *Hydrobia stagnorum*, *Cerastoderma glaucum* and *Abra ovata*); and (3) lagoons with freshwater influence (30–80% of freshwater species). According to modern analogues, the biofacies recorded in units 1, 3, 5, 7 and 9 can be associated with the lagoonal assemblage *sensu stricto*. In core M57's fossil record, the relative abundance of lagoonal macrofauna was strongly correlated with the abundance of *Cyprideis torosa* ($P_{value} = 1.116e\text{-}89$, $Lag_0 = 1$), which confirms the ecological affinities of these species (Fig. 3). Minor but persistent abundances of coastal species associated with the lagoonal assemblage emphasize marine-lagoon conditions during the deposition of Units 1, 3, 5, 7 and 9. Cross-correlation analysis also confirms the positive correlation between relative abundances of marine species and the abundance of *Cyprideis torosa* ($P_{value} = 0.0001$, $Lag_0 = +0.65$). By comparison, strontium isotopes measured on *Cyprideis torosa* shells taken from the Maryut's Holocene sequence, a lagoon located south-west of Abu Kir bay, show that variations in the abundance of lagoonal species are positively correlated with marine inputs into the lagoon's water budget (Flaux et al., 2013). The original habitats of coastal species found in core M57 include sheltered areas, infra-littoral sands, upper clean-sands and hard substrate (Fig. 3). This group, with diverse origins, was thus reworked and re-deposited within the lagoon basin. Such marine inputs could have been transported into the lagoon during high-energy events. Another possibility is that this biofacies translates proximity to a marine inlet.

By contrast, Units 4, 6 and 8 were almost entirely devoid of fauna, with the exception of a few individuals of *Cyprideis torosa* and *Hydrobia* sp. A similar biofacies was elucidated in the mid-Holocene sequence of the Maryut and Abu Qir lagoons, located south-east of Abu Qir Bay (Flaux et al., 2011). This biofacies was related to relative confined conditions, with little renewal of the lagoon water by marine inputs, according to modern Mediterranean marginal marine environments defined by Guelorget and Perthuisot (1983). Strontium isotopes measured on *Cyprideis torosa* shells taken from the Maryut's Holocene sequence confirmed that this biofacies corresponds to a lagoon depleted in seawater (10–15%; Flaux et al., 2013). Mud-rich deposits in Units 6 and 8, typical of pelagic conditions, confirm the closure of the lagoon from marine processes during their deposition. In particular, partially preserved laminated structures in Unit 6 indicate low-energy decantation processes and the absence of biological and physical reworking.

Taken as a whole, based on the paleoecological data, the M57 sequence has recorded a marginal-marine coastal environment (i.e. estuary to lagoon), characterized by alternating phases of lagoon connection and isolation from the open sea, mirrored by the abundance of *Cyprideis torosa*.

5.1.3. Paleo-coastal changes recorded in core M57

The bio-sedimentological dataset of core M57, together with six selected radiocarbon dates, allow nine successive coastal environments to be reconstructed, interpreted using modern sedimentological (El-Banna, 2008, Frihy et al., 1999, 2007) and biological (Bernasconi and Stanley, 1994) analogues from the Nile coast. The sequence translates the significant coastal changes that this area has undergone during the past ca. 7000 years.

5.1.3.1. Unit 1: estuarine sands. Unit 1 comprises lagoon fauna with minor abundances of marine species deposited in poorly sorted fine to medium sands that, according to modern analogues, are consistent with fluctuating currents on the sedimentary bottom of Abu Qir Bay. This unit is consistent with a euryhaline estuarine setting.

5.1.3.2. Unit 2: beach shoreline. Unit 2 displays well-sorted yellow sands, especially towards the top of the unit, with similar grain-size indices to modern beach sands in the study area (Fig. 2). Very low MS values translate the sorting of quartz sands, whose diamagnetic properties produce weak or negative magnetic susceptibility values (Thompson and Oldfield, 1986). Oxidized stains in the sedimentary unit confirm aerial conditions during or after deposition. The scarcity of fossils in this layer may be due to the dissolution of calcium carbonate because of subaerial weathering and decalcification. Unit 2 has therefore recorded the gradual emersion of the area, on the margin of the previous estuarine setting. Two fine layers of organic muds intercalated within the unit could be interpreted as coastal ponds punctually developed in small depressions on sandy shores (Fig. 3). The base of the unit was dated to ca. 5000 yrs cal. yr BC, marking the end of the marine transgression and the onset of deltaic accretion in this area, expressed by the progradation of coastal barriers with large wetlands on the leeward side, already described at the scale of the Nile delta coast (Stanley and Warne, 1993; Stanley and Warne, 1994).

5.1.3.3. Unit 3: marine influence. The sandy Unit 2 was subsequently buried by 20 cm of fine gray sands with moderate sorting, followed by 40 cm of sandy muds. Sand mean grain size and the sorting index values are similar to modern deposits in Abu Qir Bay, frequently reworked by waves and currents (Fig. 2). However, Unit 3′s faunal content is characterized by a dominant lagoonal assemblage with minor percentages of coastal shells, reworked from various original habitats (Fig. 3) Two inverted radiocarbon dates confirm reworking processes, notably the presence of carbonized wood dated to 16.4 cal. yr BC. Such reworking, and the submersion of Unit 2, may translate a high-energy event, which would have occurred during the fifth millennium BC.

5.1.3.4. Unit 4: marsh. The black color, lumpy structures and relatively high LOI percentages (10–45%) at 550 °C show that Unit 4 is dominated by organic inputs, consistent with peat deposits in a supratidal context. This explains the relative absence of molluscan fauna in this unit, compared to lagoonal conditions. The unit displays low MS values because organic matter has diamagnetic properties, which produce weak or negative magnetic susceptibility values (Thompson and Oldfield, 1986). The top of the layer was dated to 3.3 ± 0.2 ka cal. yr BC.

5.1.3.5. Unit 5: marine lagoon. The shelly muds of Unit 5 comprise a 0.5 m thick sequence, deposited between 3.3 and 0.9 ka cal. yr BC, yielding a mean sedimentation rate of ca. 0.2 mm yr^{-1}. This value is much lower than the mean accumulation rate of Units 2, 3 and 4 (ca. 1.3 mm yr^{-1}, Fig. 4). A decline in sediment inputs partially explains a relative increase in the biogenic component, which is around four times greater than the mean for the whole sequence. The faunal assemblage also indicates higher seawater inputs at the core site showing that the marshy shores elucidated in Unit 4 were submerged below lagoon waters. The submersion that has been used can be used as a relative sea-level index point, dated to ca. 3.3 ka cal. yr BC at 5.5 ± 0.25 m below present MSL.

5.1.3.6. Units 6 and 8: a closed lagoon. Unit 6 is 2.5 m thick and comprises dark muds, with partial conservation of laminations and is nearly devoid of fauna. Homogeneous deposition of silty clays suggests decantation depositional processes. Both units record the highest MS values in the core, ranging from 200 to 400 SI. Ghilardi and Boraik (2011) measured a similar range of MS values in late Holocene floodplain muds of the Nile (100–470 SI). High MS values were also measured in the fine sands fraction, consistent mica minerals, whose paramagnetic properties produce positive MS values. It is suggested that the mica was sorted in this pelagic environment because of its flat structure giving the mineral greater buoyancy. Bouseily and Frihy (1984) have described biotite enrichment in modern sediments deposited in the middle low-energy part of Abu Qir Bay, compared to shoreline deposits.

Furthermore, the relative absence of macro- and micro-fauna assemblages, with a very low species diversity, indicates confined conditions, with little or no connection to the sea. Unit 6 was probably part of Edku lagoon behind a sandy barrier (Chen et al., 1992). The unit was deposited between ca. 0.8 ka cal. yr BC and 0 cal. yr AD, with an apparent mean sedimentation rate of between 1.7 and 6.7 mm yr^{-1} (Fig. 5). It is the highest sedimentation rate of the sequence, translating a period of high sediment supply by the Canopic branch and subsequent progradation coast. Around Edku lagoon, archeological surveys suggest a lagoon level of 1 m above current MSL during Antiquity, which fits tightly with the geography of the ancient sites, whose settlements have functioned as part of a water-management system (Wilson, 2012). This lagoon level, above present MSL, strongly suggests that Edku lagoon was disconnected from the sea during Antiquity, consistent with the bio-sedimentological data of Unit 6.

5.1.3.7. Units 7 and 9: marine inputs into a closed lagoon. While Unit 8 is identical to Unit 6, the intercalated Unit 7 is slightly enriched in sands and is clearly differentiated by higher LOI at 950 °C and lower MS values (Fig. 3), both translating higher carbonate content because carbonates have diamagnetic properties, which produce weak or negative magnetic susceptibility values (Thompson and Oldfield, 1986). A rich lagoonal fauna characterizes the carbonate component, with the accessory presence of coastal species. The confined environment defined in units 6 and 8 was therefore temporarily interrupted by seawater inputs. The poorly sorted sand fraction of Unit 7, and the presence of coastal shells originally found in a plethora of coastal habitats, indicate periodic injections of bay sediments into the lagoon muds. The facies could thus translate the proximity of a marine inlet, or be the result of a high-energy event (a storm or a tsunami). Radiocarbon-dated seeds taken from the upper part of Unit 7 indicate that it was deposited at ca. 45 ± 80 yr. cal. AD.

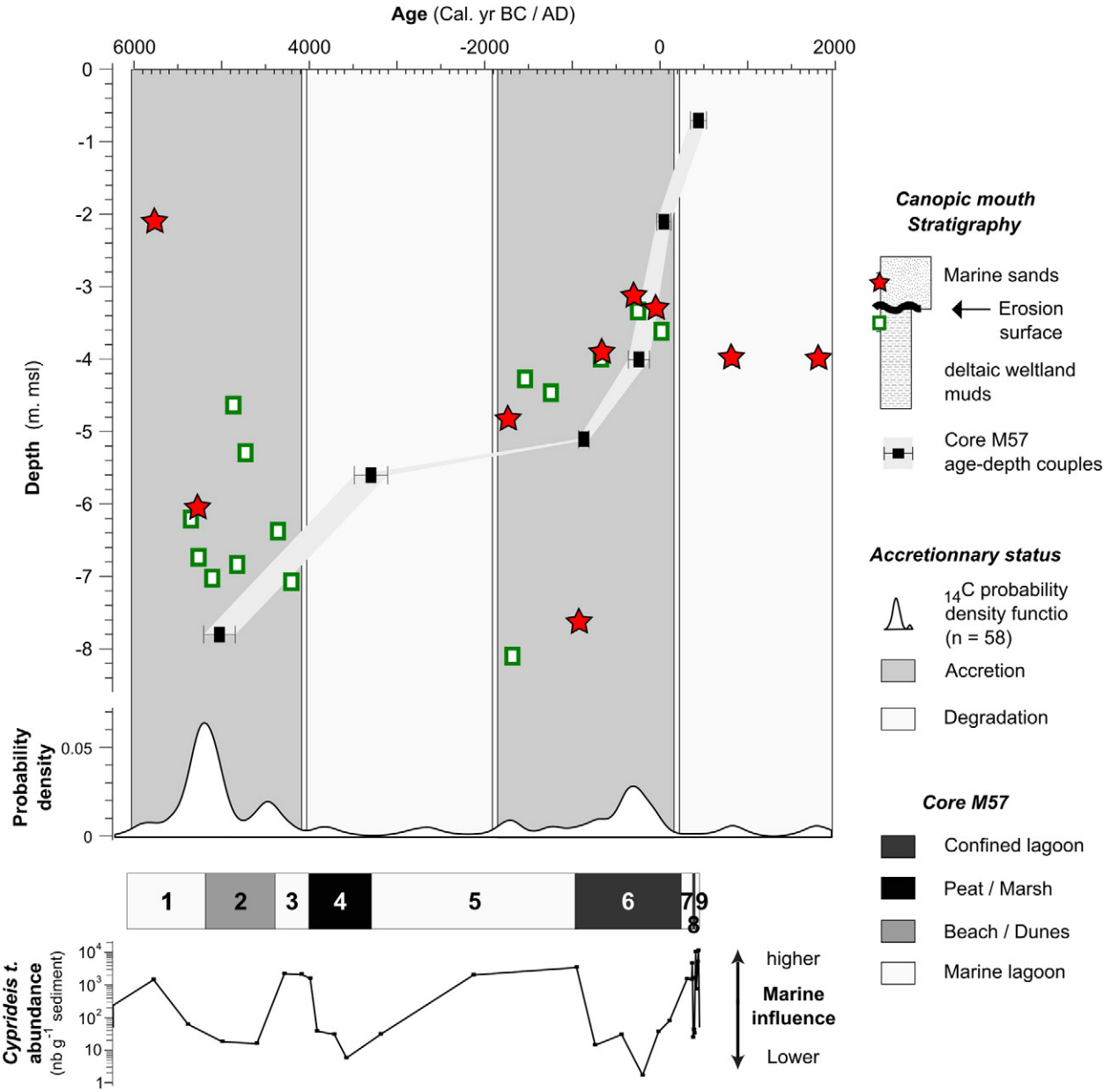

Fig. 5. Compiled age (^{14}C) - depth couplets from core M57 and Abu Qir Bay sediments (original data in Stanley, 2007). A dataset of 58 ^{14}C samples from sediment cores taken in Abu Qir Bay and core M57 were used to calculate the probability density function of ^{14}C dates, to detect phases of apparent sedimentary hiatus. Comparison with biofacies and *Cyprideis torosa* abundance from core M57 is also shown.

In a similar vein, the depositional environment attested by Unit 9 interrupts the closed lagoon identified in unit 8. The faunal assemblage of Unit 9 translates lagoonal conditions with marine inputs. The mean grain sizes and sorting indices are consistent with present infratidal environments in Abu Qir Bay (0–4 m depth; Fig. 3). An inverted date, consistent with reworking processes, was also recorded in this unit (Table 1). Once again, these marine sands, deposited above confined lagoon muds, could have recorded another high-energy event at the Canopic coast, such as storm surges, or the proximity of a marine inlet.

6. Comparison with regional data

6.1. Subsidence processes at the Canopic mouth

It was recently suggested that compaction processes have been key drivers of coastal subsidence on the Nile Delta (Becker and Sultan, 2009; Marriner et al., 2012a; Wöppelmann et al., 2013). Mean Holocene relative sea-level rise rates at and south of the Abu Qir coast were estimated to be between 1 and 2.4 mm yr^{-1} (Marriner et al., 2012a), taking into account the modeled Holocene sea-level curve for the nearby Mediterranean coast of Israel (Sivan et al., 2004). In core M57, the upper tidal peat deposit (Unit 4) indicates 3–5 m of subsidence since 3300 ± 190 years (1–1.6 mm yr^{-1}). In Abu Qir Bay, lagoon and marshy environments deposited around mean sea level between 1500 and 0 cal. yr BC were found at depths of 3 to 4.5 m below MSL (Stanley, 2007). These age-depth points yield a subsidence range of 0.8–2.3 mm yr^{-1}. Thus, core sediments from Abu Qir Bay do not show a significant vertical gap in comparison to adjacent, presently emerged, areas.

Underwater archeological excavations in Abu Qir Bay have revealed numerous undisturbed foundation structures consistent with ancient buildings (Goddio, 2007). These remains usually lie upon a hard clay layer. In the latter, the abundance of *Cyperaceae* botanic remains, brackish fauna, organic-rich deposits and cloven-hoof bovid tracks all attest to a deltaic wetland environment, deposited close to mean sea level. According to the available elevation data (Goddio, 2007), these sea-level indicators describe a relative sea-level rise of 4 to 6.5 m at East-Canopus and 5.5 to 6 m at Herakleion. Taking into account the youngest archeological artefacts and structures found at both sites, and dated from the late 7th to early 8th centuries AD, the drowned cities have been affected by an apparent relative sea-level rise ranging between 3 and 4.5 mm yr^{-1} during the last 13 centuries. Geological investigations of the underlying sediments have elucidated disturbed strata, sediment fractures and flame structures in soft sediment (Stanley et al., 2007). In Abu Qir Bay, because mean subsidence rates calculated from archeological data appear to be much greater (3–4.5 mm yr^{-1}) than regional data from sedimentary cores (1–2.5 mm yr^{-1}), we insist upon the role of heavy urban buildings upon poorly consolidated organic muds, as a main cause for the observed disparities in subsidence rates. Other such examples are known from Alexandria's ancient harbors (Goddio, 1998; Bernand and Goddio, 2002; Stanley and Toscano, 2009).

6.2. Erosion processes at the Canopic mouth

Fig. 5 depicts 23 age-depth points, compiled from 17 short cores (1.5–5.5 m thick) taken from the bottom of Abu Qir Bay (Stanley, 2007). The simplified stratigraphy of the 17 cores is characterized by a marine-sand layer, usually <1 m thick, which covers most of the present-day bottom of Abu Qir Bay. This unit lies above deltaic wetland facies including brackish peats, marshes and lagoon deposits (Stanley et al., 2007; Bernasconi et al., 2007; Fig. 5). Nine age-depth points were sampled from the base of the marine-sand layer, 14 from the top of the wetland facies.

The cumulative probability density function calculated using a dataset of 58 ^{14}C samples taken from Abu Qir's Holocene sequences (Stanley, 2007; Goddio, 2007; this study) constrains two periods with very few radiocarbon dates at 3.5–2 ka cal. yr BC and 0–2 ka cal. yr AD (Fig. 5). The apparent absence of material from these periods indicates that either: (1) no/few sediments were deposited at these times; and/or (2) these sediment tracts have been eroded since deposition. Both processes result in a very low sedimentation rate, which was also attested in the M57 record (Figs. 4 and 5).

6.2.1. Erosion between 3.5 and 2 ka cal. yr BC?

In core M57, the interface between Units 4 and 5, at ca. 3.3 ka cal. yr BC (Figs. 2 and 3), describes a marine lagoon transgression on a supratidal peat. East of the Rashid branch, at the edge of Burullus lagoon, a peat layer is capped by mollusc-rich deposits with a lagoonal ecology (Wunderlich and Andres, 1992). Chen et al. (1992) have also identified the transition from a marsh to a marine lagoon environment in the Edku region, west of the Rashid branch, during the same time period. Westward, marine inputs increased and became progressively prevalent in the Maryut lagoon after 3.5 cal. yr BC, according to a fossil and strontium isotope record (Flaux et al., 2013). These independent studies all point to higher marine influence on the northwestern Nile delta, beginning around 3.5 ka cal. yr BC. From this time up to ca. 2 ka cal. yr BC, there is a hiatus in the Abu Qir radiocarbon dataset (Fig. 5). Consistently, Unit 5 in core M57 is characterized by a very low sedimentation rate of 0.2 mm.yr^{-1} and a relatively high abundance of shell valves and debris (15–20% of the bulk sediment in comparison to a mean value of 3–4% for the whole core M57), which implies low clastic inputs. A lowering of Nile flow during this period has been widely documented, using a variety of proxies from the Nile valley, spanning source-to-sink areas, primarily mediated by a weakening of the Ethiopian Monsoon, induced by a southern shift in the mean summer position of the ITCZ (e.g. Marriner et al., 2012b and references therein). On the Abu Qir/Canopic coast, this low-Nile-flow stage is expressed by much lower sediment delivery to the coast and a probable negative sedimentary budget leading to a marine intrusion into the Canopic promontory between 3.5 and 2 ka cal. yr BC.

6.2.2. Erosion during the last 1500 years

Toussoun (1922, 1926) has reviewed documents by Greek, Roman and Arab scholars, to determine that the Canopic channel was no longer active after the 4th and before the 6th century AD. Therefore, by the 5th century AD, almost no sediments were delivered to the Canopic mouth, in line with findings from core M57, where sedimentation stops at this time. It is likely that this period has recorded the transition from accretion to shoreline retreat at the Canopic mouth, similar to the present Rashid mouth.

The Abu Qir age-depth dataset only provides two dates younger than 0 cal. yr AD (Fig. 4). As previously noted, a marine sand layer characterizes the upper stratigraphy of the bay, deposited above deltaic wetland facies. Most of the in situ archeological material was described at the interface between the upper marine sands and lower lagoon muds (Goddio, 2007). The undulating interface was found in cores between 3.2 and 7.4 m below MSL, with a deepening trend towards the east. Ages of the upper, thin, marine sands layer, display a range from ca. 6 ka cal. yr BC up to present (n = 9). This surficial layer thus incorporates old reworked material that was initially deposited much earlier. Consistently, dates from the upper lagoon muds display a range between 5.5 and 0 ka cal. yr BC (Fig. 5). Other deposits sampled immediately beneath the archeological remains were radiocarbon dated between 0.7 ka cal. yr BC and 0.1 ka cal. yr AD (n = 9), although three samples were much older, dated between 4.3 and 5.7 ka cal. BC (Goddio, 2007). These observations clearly depict an undulating surface, up to 4 m in amplitude, resulting from the erosion of various thicknesses of the lagoon muds. Sand fractions of some of these eroded lagoonal sediments may have fed the present upper sand layers and would explain its wide age range.

Archeological investigations also attest to strong marine erosion on the Abu Qir bottom. For example, the configuration of East-Canopus' remains is markedly contrasted. The western side comprises a plateau

around 3.5–4 m below MSL, while the eastern side lies on a slope going down to 6 m below MSL further east (Goddio, 2007, their Fig. 2.2). The archeological structures on the western side are clearly best preserved. The foundation courses, with some elevation courses still preserved, clearly delineate in situ buildings, buried beneath 1 to 2 m of marine sands. Conversely, on the eastern side, scattered archeological material was found, intermingled with fragments of Pharaonic, Ptolemaic and Roman statuary (Goddio, 2007, p. 35). This taphonomy probably resulted from the dismantling of the stratified deposits through erosion and removal of fine sediments at the eastern edge of East-Canopus.

The protection and stabilization of the southwestern Abu Qir shores have a long history. A relict dike was described on the western coastline of Abu Qir Bay by early 19th century AD engineers from the French Expedition in Egypt (Jacotin, 1818). Seawards, submerged (older?) stone dikes were also observed by Toussoun (1934) and Goddio (2007, p.23). A 10-km-long quarry-stone barrier was built in 1830 and reinforced in 1980 on the southern shoreline of Abu Qir Bay (Frihy et al., 2010). Frihy and Komar (1993) and Frihy et al. (2007) conducted measurements of beach profiles and described the retreat of the bay's western flank at a rate of 0–2 m yr^{-1}, from 1971 to 1990. Within the bay itself, bottom currents displace surface sediments laterally (Frihy et al., 1994) and have smoothed the submerged Canopic promontory, 80% of whose surface ranges between 5.5 and 6.5 m below MSL (Stanley et al., 2004). The study by Bouseily and Frihy (1984) summarizes 1500 years of coastal erosion at the Canopic mouth. Their analysis shows that modern beach sediments on the western side of Abu Qir Bay are coarser, more poorly sorted, more negatively skewed and more enriched in heavy minerals than in other parts of the coastal bay. These sedimentological characteristics have been attributed to reworking of the relict bottom sediments of the Nile's paleo-Canopic mouth. A similar pattern has been described for the ancient Sebennitic mouth on the central delta coast (Frihy and Komar, 1993; Frihy et al., 1994; Frihy and Lotfy, 1994).

This series of arguments demonstrates that erosion has been an important process in shaping Abu Qir Bay. The Canopic mouth mainly evolves like the modern Rashid promontory, when the mouth ceased to be a depositional center and became a source of sediments that were redistributed by coastal currents. Erosion of the marshy lagoonal sequence deposited in the context of the Canopic estuary, in some places up to 4 m thick, was also responsible for the lowering of the promontory and archeological remains. By comparison, the outer harbor of Roman Arles, a former estuarine lagoon located behind an underwater bank at the mouth of the Saint Ferréol branch on the Rhône delta (France), was found 8–9 m below MSL, in the form of aligned limestone blocks related to possible harbor buildings, anchors and waste disposal (Long and Duperron, 2011). Interestingly, the stratigraphy of the site is very similar to the one described in Abu Qir Bay: the remains lie upon stiff lagoon muds, buried below a thin surface layer of shelly sands. The mouth bar was reconstructed following the discovery of 14 wrecks, distributed in a clear arc form. The wrecks currently lie 12 to 14 m below MSL, and between 1 and 3 km seaward of the present shoreline (Long and Duperron, 2011). Here, the evolution of the mouth bar was related to erosion processes after the progressive infilling of the corresponding channel between the 2nd and 6th centuries AD (Provansal et al., 2003; Vella et al., 2005). We stress that calculations of total subsidence in Abu Qir Bay cannot be solely related to sediment failures (Stanley et al., 2004; Stanley et al., 2004) and must include sediment removal by erosion.

6.3. The role of high-energy events

Historian Ammianus Marcellinus documented the devastating effects of a tsunami hitting Alexandria (Guidoboni et al., 1994, p. 267–268) and the Nile delta in 365 CE (Shaw et al., 2008, Stiros, 2010). Investigating the paleo-coast of Alexandria, however, Goiran et al. (2005) found a homogeneous sequence of harbor muds deposited throughout the Roman period, without any sedimentological impact of the destructive wave. Nevertheless, Goiran et al. (2005) and Goiran (2012) documented a deposit of coarse and reworked material, including allochtonous macrofauna, attributed to another tsunami known to have affected Alexandria in 881 cal. yr AD. Stanley and Warne (1993) reconstructed the late Quaternary history of the Nile coast through the detailed study of 86 core sections. Surprisingly, no tsunami deposits or related impacts were found. Tracking the wave impact, Stanley and Jorstad (2005) have, however, described a major sedimentary hiatus in the upper part of Alexandria's harbor stratigraphy. They ascribe this hiatus to important erosion of the harbor floor by high-energy wave surges. In Abu Qir Bay, Stanley et al. (2007) suggest that a tsunami wave could have triggered mud liquefaction and strata failure, but no tsunamites were identified in cores taken from the bay.

In core M57, Unit 3 indicates the deposition of sandy muds above beach sands. Presence of coastal fauna at least partially translates the marine origin of the material. Furthermore, two inverted dates and a carbonized wood fragment dating to the last glacial maximum attest to important reworking processes. In the upper sequence of core M57, Units 7 and 9 recorded the intrusion of coastal sands within a closed lagoon and Unit 9 also comprises old reworked material. These observations show changes in the depositional environment and reworking processes that may be attributed to high-energy coastal events such as storm surges or tsunamis. Using ancient textual sources, Goiran (2012) reported eight high-energy waves (tsunamis or strong storms) that have affected the coast of Alexandria during the last 2000 years. The oldest event was reported at 23 $\pm$ 3 cal. yr. AD and the second was attributed to the notorious 365 CE tsunami. According to the M57 age model, Units 7 and 9 were respectively deposited during the 1st century AD and during the 3rd–5th centuries AD. They could have thus partially recorded the sedimentary imprint of two high-energy events on the Canopic coast. However, these units could also correspond to a marine inlet environment. The identification of clear geomorphological impacts resulting from high-energy events on the Nile coast remains a challenge for future geoarcheological on the Nile delta (e.g. Morhange et al., 2013).

6.4. Was Herakleion deserted because of coastal subsidence and erosion?

Extensive archeological surveys conducted on the northwestern Nile delta have highlighted how the region's fluvial and lagoonal geography clearly dictated the network of settlements during Antiquity (de Cosson, 1935; Empereur and Picon, 1998; Empereur, 1998; Rodziewicz, 1998, 2002; Wilson and Grigoropoulos, 2009; Wilson, 2010; Khalil, 2010; Blue and Khalil, 2010; Blue et al., 2011; Boussac and El-Amouri, 2010; Pichot, 2010; Wilson, 2012; Flaux, 2012; Thomas, 2014). As a whole, waterflow and groundwater resources were dependent upon the Canopic branch. By the 7th century AD, however, occupation of the northwestern delta declined sharply (Thomas, 2014). From the very beginning of the Islamic period, Alexandria lost its standing as the first town of Egypt as well as the country's main maritime and lake harbors (Rodziewicz, 2002). When commercial roads towards Constantinople and the Eastern Roman Empire sharply ceased, industrial farms based on this economy were rapidly abandoned (Décobert, 2002). Cooper (2009) demonstrated that the grain tribute was redirected from the Eastern Mediterranean to the Rashidun Caliphate in Egypt, and to Mecca and Medina. Because its activities were closely linked to the export of Egyptian grain towards the Mediterranean, Naukratis, which had been established on the flank of the Canopic branch in the late 7th century BC as a base for Greek and Eastern Mediterranean traders, also declined by the 7th century AD (Thomas, 2014). In this context, it is not surprising that Herakleion and East-Canopus, as East-Mediterranean trade harbors at the mouth of the Canopic, were apparently also deserted by the 7th century AD.

7. Conclusion

The Nile's promontories constitute sensitive coastal areas that respond rapidly to changes in relative sea level and sediment supply. Bio-sedimentological data from core M57, drilled at the edge of the former Canopic promontory, have recorded four stages of marine incursion at ca. 4.4 ka cal. yr BC, 3.3 ka cal. yr BC, ca. 0.1 ka cal. AD and 0.3–0.4 ka cal. yr AD, which interrupt the general progradation trend of the Nile coast in this area. The marine influence recorded at 3.3 ka cal. yr BC was stable until 0.8 ka cal. yr BC and is reflected by an apparent sedimentary hiatus attested in sub-surface sediments from Abu Qir between 3.5 and 2 ka cal. yr BC. The hiatus indicates a negative sedimentary budget at the Canopic mouth and may translate the coastal response to climatic aridification of the Nile catchment during this period. Sediment supply was once again high between 2 cal. yr BC and 0.5 ka cal. yr AD, which led to the accretion and subsequent occupation of the Canopic lobe. After 0.5 ka cal. yr BC, a second stage is recorded where erosion and reworking processes dominated at the Canopic mouth, which led, in conjunction with long-term compaction and the failure of unconsolidated organic-rich sediments, to the lowering of the Canopic's promontory, whose relic surface now lies 6.5–5.5 m below MSL, and the persistent retreat of Abu Qir's southwestern coast up to present day. This second stage of negative sedimentary budget at the Canopic mouth fits tightly with the absence of historical references to the Canopic mouth from the 5th century AD onwards. Like the present Rashid promontory, the accretion and degradation status of the Canopic mouth was primarily controlled by sediment supply.

Because relative sea-level indicators, from core sediments in Abu Qir Bay and in adjacent areas presently still emerged, do not show a significant vertical gap, there is no evidence for failure of the Canopic promontory as a whole. However, as mean subsidence rates calculated from archeological data appear much greater than regional stratigraphic data, the role of compaction processes by heavy urban structures built upon poorly consolidated organic muds would have been significant.

There is no clear evidence that the submersion of Herakleion and East-Canopus was sudden and "catastrophically" forced the population to leave. Despite the 365 CE tsunami, possibly recorded in core M57 by an intrusion of marine sediments within lagoonal muds (Unit 9), and although the Canopic flow reaching the mouth was already low by the 5th century AD, inducing silting-up of the channel, coastal erosion and the possible mobility of submarine mouth bars by comparison with the modern Rashid promontory (Frihy and Lawrence, 2004), archeology from the late Roman period, i.e. from the 5th to the 7th century AD, is very well represented in Abu Qir Bay (Goddio, 2007). The maritime cities, open to the Eastern Mediterranean's economy, declined in tandem with the northwestern delta occupation, during the 7th century AD, in response to wider political and economic changes in the context of the Arabic conquest. This is not to say that the coastal cities were not affected by high-energy events, such as rapid land failure, tremors or tsunamis. However, it remains a challenge for coastal geoarcheology to examine both geomorphological and societal response to catastrophic events, in part because of the daily to weekly resolution required. Ambraseys (2005) claimed that "Perhaps it is one of the most interesting findings that the lasting effects of major earthquakes over the last 25 centuries in the eastern Mediterranean region would not seem to have been significant [for coastal societies]. Soon after a damaging or destructive earthquake, vested interests invariably led people to act once again with disregard for the prospect of further such calamities, and they still do". This conclusion may also explain the longevity of both Herakleion and East-Canopus, founded in the 6–7th centuries BC at the Canopic mouth.

Acknowledgments

This research was funded by the project GEOMAR (ANR-12-SENV-0008-03) managed by the French National Research Agency (ANR), Artemis INSU (Institut National des Sciences de l'Univers), Egide Imhotep (project 25688PG), IUF, MISTRALS/PALEOMEX and Labex OT-Med (ANR-11-LABEX-0061) funded by the "Investissements d'Avenir", (A*Midex project, ANR-11-IDEX-0001-02).

References

Ambraseys, N., 2005. Archaeoseismology and neocatastrophism. Seismol. Res. Lett. 76 (5), 560–564.
Anthony, E.J., 2009. Shore Processes and their Palaeoenvironmental Applications. Developments in Marine Geology vol. 4. Elsevier, Amsterdam.
Anthony, E.J., Marriner, N., Morhange, C., 2014. Human influence and the changing geomorphology of Mediterranean deltas and coasts over the last 6000 years: from progradation to destruction phase? Earth Sci. Rev. 139, 336–361.
Becker, R.H., Sultan, M., 2009. Land subsidence in the Nile delta: inferences from radar interferometry. The Holocene 19 (6), 949–954.
Bernand, A., Goddio, F., 2002. L'Egypte Engloutie - Alexandrie. Arcperiplus Publishing, London.
Bernasconi, M.P., Stanley, D.J., 1994. Molluscan biofacies and their environmental implications, Nile delta lagoons, Egypt. J. Coast. Res. 10 (2), 440–465.
Bernasconi, M.P., Melis, R., Pugliese, N., Stanley, J.-D., Bandelli, A., 2007. Faunal Analyses in the Interpretation of the Submergence of Substrates beneath Herakleion and East Canopus. In: Stanley, J.D. (Ed.), Underwater Archaeology in the Canopic Region in Egypt. Oxford Centre for Maritime Archaeology, Monograph 2, Oxford, pp. 59–86.
Blue, L., Khalil, E. (Eds.), 2010. Lake Mareotis: Reconstructing the Past. Proceedings of the International Conference on the Archaeology of the Mareotic Region, Bar International Series 2113, Oxford.
Blue, L., Khalil, E., Trakadas, A. (Eds.), 2011. A Multidisciplinary Approach to Alexandria's Economic Past: The Lake Mareotis Research Project. Bar International Series 2285, Oxford.
Bouseily, A.M., Frihy, O.E., 1984. Textural and mineralogical evidence denoting the position of the mouth of the old Canopic Nile branch on the Mediterranean coast, Egypt. J. Afr. Earth Sci. 2 (2), 103–107.
Boussac, M.F., El-Amouri, M., 2010. The Lake Structures at Taposiris. In: Blue, L., Khalil, E. (Eds.), Lake Mareotis: Reconstructing the Past. Proceedings of the International Conference on the Archaeology of the Mareotic Region. Bar International Series 2113, Oxford, pp. 87–105.
Chen, Z., Warne, A.G., Stanley, J.D., 1992. Late quaternary evolution of the northwestern Nile Delta between the Rosetta promontory and Alexandria, Egypt. J. Coast. Res. 8 (3), 527–561.
Church, J.A., White, N.J., Konikow, L.F., Domingues, C.M., Cogley, J.G., Rignot, E., Gregory, J.M., van den Broeke, M.R., Monaghan, A.J., Velicogna, I., 2011. Revisiting the Earth's sea-level and energy budgets from 1961 to 2008. Geophys. Res. Lett. 38 (18), 1–8.
Coleman, J.M., Roberts, H.H., Stone, G.W., 1998. Mississippi river delta: an overview. J. Coast. Res. 14 (3), 698–716.
Cooper, J.P., 2009. Egypt's Nile–Red Sea Canal: Chronology, Location, Seasonality and Function. In: Blue, L., Cooper, J., Thomas, R.I., Whitewright, R.J. (Eds.), Connected Hinterlands: Proceedings of Red Sea Project IV. BAR International Series 2052, Oxford, pp. 195–210.
de Cosson, A., 1935. Mareotis, being a Short Account of the History and Ancient Monuments of Thenorth-Western Desert of Egypt and of Lake Mareotis. Country Life Ltd., London.
Décobert, C., 2002. Maréotide médiévale. Des bédouins et des chrétiens. In: Décobert, C. (Ed.), Etudes Alexandrines 8, Alexandrie Médiévale 2. IFAO, Le Caire, pp. 127–167.
Doneddu, M., Trainito, E., 2005. Conchiglie del Mediterraneo. Il Castello, Trezzano sul Naviglio.
El-Banna, M.M., 2008. Vulnerability and fate of a coastal sand dune complex, Rosetta-Edku, northwestern Nile Delta, Egypt. Environ. Geol. 54, 1291–1299.
Empereur, J.-Y., 1998. Alexandrie redécouverte. Fayard/Stock, Paris.
Empereur, J.-Y., Picon, M., 1998. Les Ateliers d'amphores Du Lac Mariout. In: Empereur, J.-Y. (Ed.), Commerce et Artisanat Dans l'Alexandrie hellénistique et Romaine. Bulletin de Correspondance Hellénique, Athènes, pp. 75–91.
Flaux, C., 2012. Holocene Coastal Palaeo-Environment of Maryut Lake in the Northwestern Nile Delta, Egypt. (PhD Thesis). Aix-Marseille University.
Flaux, C., Morhange, C., Marriner, N., Rouchy, J.-M., 2011. Bilan hydrologique et biosédimentaire de la lagune du Maryût (delta du Nil, Egypte) entre 8000 et 3200 ans cal. B.P. Géomorphologie 17 (3), 261–278.
Flaux, C., Claude, C., Marriner, N., Morhange, C., 2013. A 7500 years strontium isotope record from the northwestern Nile delta (Maryut lagoon, Egypt). Quat. Sci. Rev. 78, 22–33.
Folk, R.L., 1966. A review of grain-size parameters. Sedimentology 6, 73–93.
Frihy, O.E., Dewidar, K.M., 2003. Patterns of erosion/sedimentation, heavy mineral concentration and grain size to interpret boundaries of littoral sub-cells of the Nile Delta, Egypt. Mar. Geol. 199, 27–43.
Frihy, O.E., Komar, P.D., 1993. Long-term changes and the concentration of heavy minerals in beach sands of the Nile delta, Egypt. Mar. Geol. 115, 253–261.
Frihy, O.E., Lawrence, D., 2004. Evolution of the modern Nile delta promontories: development of accretional features during shoreline retreat. Environ. Geol. 46, 914–931.
Frihy, O.E., Lotfy, M.F., 1994. Mineralogic evidence for the remnant Sebennitic promontory on the continental shelf off the central Nile delta. Mar. Geol. 117, 187–194.

Frihy, O.E., Moussa, A.A., Stanley, D.-J., 1994. Abu Qir, a sediment sink off the northwestern Nile delta, Egypt. Mar. Geol. 12, 199–211.
Frihy, O.E., El-Askary, M.A., Deghidy, E.M., Moufaddal, W.M., 1999. Differentiating fluvio-marine depositional environments in the Nile delta using textural and compositional components. J. Afr. Earth Sci. 28, 599–618.
Frihy, O.E., Hassan, M.S., Deabes, E.A., Abd El-Moniem, A.B., 2007. Seasonal wave changes and the morphodynamic response of the beach-inner shelf of Abu Qir Bay, Mediterranean coast, Egypt. Mar. Geol. 247 (3–4), 145–158.
Frihy, O.E., Deabes, E.A., Shereet, S.M., Abdalla, F.A., 2010. Alexandria-Nile delta coast, Egypt: update and future projection of relative sea-level rise. Environ. Earth Sci. 61, 253–273.
Ghilardi, M., Boraik, M., 2011. Reconstructing the holocene depositional environments in the western part of Ancient Karnak temples complex (Egypt): a geoarchaeological approach. J. Archaeol. Sci. 38, 3204–3216.
Goddio, F. (Ed.), 1998. Alexandria: The Submerged Royal Quarters. Periplus Publishing London Ltd., London.
Goddio, F., 2007. The Topography and Excavation of Heracleion-Thonis and East Canopus (1996-2006). Underwater Archaeology in the Canopic Region (Oxford Centre for Maritime Archaeology Monograph 1). OCMA, Oxford.
Goiran, J.-P., 2001. Recherches géomorphologiques dans la région littorale d'Alexandrie en Egypte. (PhD Thesis). Aix-Marseille University.
Goiran, J.-P., 2012. Caractérisation d'un dépôt de Tsunami Dans le Port Antique d'Alexandrie Par l'étude Exoscopique Des Quartz: Apports et Limites de la Méthode. In: Rébé-Marichal, I., Laurenti, A., Boehm, I., Goiran, J.-P. (Eds.), Archéosismicité & Tsunamis en Méditerranée, Approches croisées. Editions APS, Perpignan, pp. 157–190.
Goiran, J.-P., Marriner, N., Morhange, C., Abd el-Maguid, M., Espic, K., Bourcier, M., Carbonel, P., 2005. Evolution géomorphologique de la façade maritime d'Alexandrie (Egypte) au cours des six derniers millénaires. Méditerranée 104, 61–65.
Guelorget, O., Perthuisot, J.-P., 1983. Le Domaine Paralique: Expressions géologiques, Biologiques et économiques du Confinement. Travaux du Laboratoire de Géologie. Ecole Normale Supérieure, Paris.
Guidoboni, E., Comastri, A., Traina, G., 1994. Catalogue of Ancient Earthquakes in the Mediterranean Area up to the 10th Century. Istituto Nazionale di Geofisica, Bologna.
Heiry, O., Lotter, A.F., Lemcke, G., 2001. Loss on ignition as a method for estimating organic and carbonate content in sediments: reproducibility and comparability of results. J. Paleolimnol. 25, 101–110.
Jacotin, P.M., 1818. Carte Topographique de l'Egypte et de Plusieurs Parties Des Pays Limitrophes. Paris, Planche 37, édition impériale.
Khalil, E., 2010. The Sea, the River and the Lake: All the Waterways Lead to Alexandria. Bollettino Du Archaeologia on Line 1, vol. speciale B/B7/5, pp. 33–48.
Long, L., Duperron, G., 2011. Recherches Sous-Marines Au Large Des Saintes-Maries-De-La-Mer (Bouches-Du-Rhône): Sur Les Traces de l'avant-Port Maritime d'Arles. Actes Du Congrès d'Arles. SFECAG, Arles, pp. 97–118.
Macklin, M.G., Toonen, W.H.J., Woodward, J.C., Williams, M.A.J., Flaux, C., Marriner, N., Nicoll, K., Verstraeten, G., Spencer, N., Welsby, D., 2015. A new model of river dynamics, hydroclimatic change and human settlement in the Nile Valley derived from meta-analysis of the Holocene fluvial archive. Quat. Sci. Rev. 130, 109–123.
Marriner, N., Flaux, C., Kaniewski, D., Morhange, 2012a. The Nile delta's sinking past: quantifiable links with Holocene compaction and climate-driven changes in sediment supply? Geology 41, 987–990.
Marriner, N., Flaux, C., Kaniewski, D., Morhange, C., Leduc, G., Moron, V., Chen, Z., Gasse, F., Empereur, J.-Y., Stanley, J.-D., 2012b. ITCZ and ENSO-like pacing of Nile delta hydrogeomorphology during the Holocene. Quat. Sci. Rev. 45, 73–84.
Marriner, N., Flaux, C., Morhange, C., Stanley, J.-D., 2013. Tracking Nile delta vulnerability to Holocene change. PLoS One 8 (7), 691–695.
Morhange, C., Salamon, A., Bony, G., Flaux, C., Galili, E., Goiran, J.-P., Zviely, D., 2013. Geoarchaeology of Tsunamis and the Revival of Neocatastrophism in the Eastern Mediterranean. In: Nigro, L. (Ed.), Rome "La Sapienza" Studies on the Archaeology of Palestine & Transjordan. ROSAPAT 11, Rome, pp. 61–81.
Nicholls, R.J., Wong, P.P., Burkett, V.R., Codignotto, J.O., Hay, J.E., McLean, R.F., Ragoonaden, S., Woodroffe, C.D., 2007. Coastal Systems and Low-Lying Areas. In: Parry, M.L., et al. (Eds.), Climate Change 2007: Impacts, Adaptation and Vulnerability, Contribution of Working Group II to the Fourth Assessment Report of the Intergovernmental Panel on Climate Change. Cambridge University Press, Cambridge, pp. 315–356.
Pérès, J.-M., 1982. Major Benthic Assemblages. In: Kinne, O. (Ed.), Marine Ecology, Part 1 vol. 5. Wiley, Chichester, pp. 373–522.
Péres, J.-M., Picard, J., 1964. Nouveau Manuel de Bionomie Benthique de La Mer Méditerranée. Periplus, Marseille.
Pichot, V., 2010. Marea Peninsula: Occupation and Workshop Activities on the Shores of Lake Mariout in the Work of the Centre d'études Alexandrines. In: Blue, L., Khalil, E. (Eds.), Lake Mareotis: Reconstructing the Past. Proceedings of the International Conference on the Archaeology of the Mareotic Region. Bar International Series 2113, Oxford, pp. 57–66.
Poppe, G.T., Goto, Y., 1991. European Seashells. vol. I. Verlag Christa Hemmen, Wiesbaden.
Poppe, G.T., Goto, Y., 1993. European Seashells. vol. II. Verlag Christa Hemmen, Wiesbaden.
Provansal, M., Vella, C., Arnaud-Fassetta, G., Sabatier, F., Maillet, G., 2003. Role of fluvial sediment inputs in the mobility of the Rhône delta coast (France). Géomorphologie 9 (4), 271–282.
Reimer, P.J., Baillie, M.G.L., Bard, E., Bayliss, A., Beck, J.W., Blackwell, P.G., Bronk Ramsey, C., Buck, C.E., Burr, G.S., Edwards, R.L., Friedrich, M., Grootes, P.M., Guilderson, T.P., Hajdas, I., Heaton, T.J., Hogg, A.G., Hughen, K.A., Kaiser, K.F., Kromer, B., McCormac, F.G., Manning, S.W., Reimer, R.W., Richards, D.A., Southon, J.R., Talamo, S., Turney, C.S.M., Van der Plicht, J., Weyhenmeyer, C.E., 2009. IntCal09 and Marine09 radiocarbon age calibration curves, 0–50,000 years cal BP. Radiocarbon 51 (4), 1111–1150.
Rodziewicz, M., 1998. From Alexandria to the West by Land and by Waterways. In: Empereur, J.-Y. (Ed.), Commerce et Artisanat Dans l'Alexandrie hellénistique et Romaine. Bulletin de Correspondance Hellénique, Athènes.
Rodziewicz, M., 2002. Mareotic Harbours. Alexandrie Médiévale 2. Etudes Alexandrines 8, pp. 1–22.
Shaw, B., Ambraseys, N.N., England, P.C., Floyd, M.A., Gorman, G.J., Higham, T.F.G., Jackson, J.A., Nocquet, J.-M., Pain, C.C., Piggott, M.D., 2008. Eastern Mediterranean tectonics and tsunami hazard inferred from the AD 365 earthquake. Nat. Geosci. 1, 268–276.
Sivan, D., Lambeck, K., Toueg, R., Raban, A., Porath, Y., Shirman, B., 2004. Ancient coastal wells of Caesarea Maritima, Israel, an indicator for relative sea level changes during the last 2000 years. Earth Planet. Sci. Lett. 222, 315–330.
Stanley, J.-D., 1996. Nile delta: extreme case of sediment entrapment on a delta plain and consequent coastal land loss. Mar. Geol. 129, 189–195.
Stanley, J.-D., 2005a. Growth faults, a distinct carbonate-siliciclastic interface and recent coastal evolution, NW Nile Delta, Egypt. J. Coast. Res. 42, 309–318.
Stanley, J.D., 2005b. Submergence and burial of ancient coastal sites on the subsiding Nile delta margin, Egypt. Méditerranée 1 (2), 65–73.
Stanley, J.D. (Ed.), 2007. Underwater Archaeology in the Canopic Region in Egypt. Oxford Centre for Maritime Archaeology, Oxford.
Stanley, J.-D., Jorstad, T.F., 2005. The 365 A.D. Tsunami Destruction of Alexandria, Egypt: Erosion, Deformation of Strata and Introduction of Allochthonous Material. Geological Society of America, Annual Meeting, Salt Lake City.
Stanley, D.J., Toscano, M.A., 2009. Ancient archaeological sites buried and submerged along Egypt's Nile delta coast: gauges of Holocene delta margin subsidence. J. Coast. Res. 25 (1), 158–170.
Stanley, J.-D., Warne, A.G., 1993. Nile delta: recent geological evolution and human impact. Science 260, 630–634.
Stanley, J.D., Warne, A.G., 1994. Worldwide initiation of Holocene marine deltas by deceleration of sea-level rise. Science 265, 228–231.
Stanley, D.J., Goddio, F., Schnepp, G., 2001. Nile flooding sank two ancient cities. Nature 412, 293–294.
Stanley, D.J., Warne, A.G., Schnepp, G., 2004a. Geoarchaeological interpretation of the Canopic, largest of the relict Nile Delta distributaries, Egypt. J. Coast. Res. 20 (3), 920–930.
Stanley, J.-D., Goddio, F., Jorstad, T.F., Schnepp, G., 2004b. Submergence of ancient Greek cities off Egypt's Nile delta – a cautionary tale. Geol. Soc. Am. 14, 4–10.
Stanley, J.D., Schnapp, G., Jorstad, T., 2007. Submergence of Archaeological Sites in Aboukir Bay, the Result of Gradual Long-Term Processes plus Catastrophic Events. In: Stanley, J.D. (Ed.), Underwater Archaeology in the Canopic Region in Egypt. Oxford Centre for Maritime Archaeology, Oxford.
Stewart, I., Morhange, C., 2009. Coastal Geomorphology and Sea-Level Change. In: Woodward, J. (Ed.), The Physical Geography of the Mediterranean. Oxford University Press, Oxford.
Stiros, S.C., 2010. The 8.5+ magnitude, AD365 earthquake in Crete: coastal uplift, topography changes, archaeological and historical signature. Quat. Int. 216, 54–63.
Syvitski, J.P.M., Kettner, A.J., Overeem, I., Hutton, E.W.H., Hannon, M.T., Brakenridge, G.R., Day, J., Vérésmarty, C., Saito, Y., Giosan, L., Nicholls, R.J., 2009. Sinking Deltas Due to Human Activities. Nature Geoscience 2 pp. 681–686.
Thomas, R., 2014. Roman Naukratis and its Alexandrian context. Br. Mus. Stud. Anc. Egypt Sudan 21, 193–218.
Thompson, R., Oldfield, F., 1986. Environmental Magnetism. George Allen & Uniwin, London.
Toussoun, O., 1922. Mémoires Sur Les Anciennes Branches Du Nil, époque Ancienne. Mémoire de l'Institut d'Egypte 4, Le Caire.
Toussoun, O., 1926. La géographie de l'Egypte à l'époque Arabe. Tome 1, Partie 1, Mémoire de La Société Royale Archéologique d'Alexandrie, Tome 8, Le Caire.
Toussoun, O., 1934. Les ruines sous-marines de la baie d'Aboukir. Bull. Soc. R. Archéol. Alexandrie 29, 342–352.
Vacchi, M., Marriner, N., Morhange, C., Spada, G., Fontana, A., Rovere, A., 2016. Multiproxy assessment of Holocene relative sea-level changes in the western Mediterranean: sea-level variability and improvements in the definition of the isostatic signal. Earth-Sci. Rev. 155, 172–197.
Vella, C., Fleury, T.-J., Raccasi, G., Provansal, M., Sabatier, F., Bourcier, M., 2005. Evolution of the Rhône delta plain in the Holocene. Mar. Geol. 222–223, 235–265.
Wilson, P., 2010. Recent Survey Work in the Southern Mareotis Area. In: Blue, L., Khalil, E. (Eds.), Lake Mareotis: Reconstructing the Past. Proceedings of the International Conference on the Archaeology of the Mareotic Region. Bar International Series 2113, Oxford.
Wilson, P., 2012. Waterways, settlements and shifting power in the northwestern Nile Delta. Water Hist. 4 (1), 95–117.
Wilson, P., Grigoropoulos, D., 2009. The West Nile Delta Regional Survey, Beheira and Kafr Esh-Sheikh Provinces. Egypt Exploration Society, London.
Wöppelmann, G., Le Cozannet, G., de Michele, M., Raucoules, D., Cazenave, A., Garcin, M., Hanson, S., Marcos, M., Santamaría-Gómez, A., 2013. Is land subsidence increasing the exposure to sea level rise in Alexandria, Egypt ? Geophys. Res. Lett. 40 (12), 2953–2957.
Wunderlich, J., Andres, W., 1992. Late Pleistocene and Holocene Evolution of the Western Nile Delta and Implications for its Future Development. In: Brückner, H., Radtke, U. (Eds.), Von Der Nordsee Bis Zum Indischen Ozean. Erdkundliches Wissen 105, Stuttgart.